Effect of Polythalamide Material Leachate on Platinum-alloy Polymer Electrolyte Membrane Performance

Christian T. Carey

Office of Science, Science Undergraduate Laboratory Internship Program
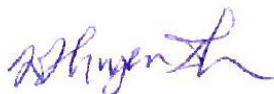
University of South Carolina, Columbia, SC

National Renewable Energy Laboratory

Golden, Colorado

May 13, 2016

Participant: <u>Christian T. Carey</u>

Research Advisor: <u>Dr. Huyen Dinh</u>

ABSTRACT

Polymer electrolyte membrane (PEM) fuel cells produce electricity, with only water as the exhaust, from the electrochemical reaction of hydrogen fuel and oxygen from the air. It is a promising technology for transportation applications as it would greatly reduce greenhouse gas emissions. To enable commercialization of fuel cells, it is important to reduce their cost while maintaining their performance and durability. Using Pt-alloy catalysts is one way to lower the fuel cell cost. However, low loading Pt-alloy catalysts are more susceptible to contaminants and can result in lower performance and shorter lifetime. This work examines the effect of a leachate solution from a polythalamide (PPA) structural material on a platinum-alloy cathode. Diagnostics used to understand the poisoning effect include fuel cell polarization curves (VIR), cyclic voltammetry (CV), and electrochemical impedance spectroscopy (EIS). EIS data were analyzed in depth in order to better understand the poisoning mechanism of the PPA leachate. The results showed that the PPA contaminant mixture resulted in a performance loss of 21 mV but the fuel cell was able to recover via self-induced recovery as well as potential cycling.

I. INTRODUCTION

Polymer Electrolyte Membrane Fuel Cells (PEMFCs) produce electricity using only oxygen from the air and hydrogen fuel. The PEM's role in the membrane electrode assembly (MEA) is to transport protons from anode to cathode while electrons are transferred through an external circuit. MEAs generally contain a PEM, an anode catalyst layer, a cathode catalyst layer, gas diffusion layers, flow fields, and current collectors. Catalyst layers are constructed by dispersing Pt nanoparticles onto carbon supports, and are connected by a Nafion® ionomer. An MEA with a higher Pt loading can increase the reaction rate and efficiency of a fuel cell, but it also increases the cost. The Department of Energy has set a 2020 goal for fuel cells to perform for 5000 hours at a cost of $40/kW[1].

New MEAs with lower loading of Pt and Pt-alloys have been developed to lower fuel cell cost. To determine how contaminants affect the performance of these new cathode catalysts, the Fuel Cells R&D team at the National Renewable Energy Laboratory (NREL) carried out a series of *in-situ* measurements before, during, and after contaminant infusion.

The diagnostics performed on these MEAs included polarization curves (VIR), cyclic voltammetry (CV), and electrochemical impedance spectroscopy (EIS). From these techniques, the overall fuel cell performance, the electrochemically active surface area (ECA), as well as characterization of resistance in the catalyst layer and the kinetics of the oxygen reduction reaction were determined. The results allow a better understanding of the contamination and recovery mechanisms of fuel cells.

The contaminant used in this study was a PPA leachate solution, aged and provided by General Motors (GM). PPA is a relatively low cost structural material that can be used in fuel cell systems. The PPA leachate contains a mixture of anions, cations, inorganics, and organics[2]. Understanding how these low loading MEAs perform in the presence of system contaminants allows the selection of clean materials for fuel cell systems that reduce operation cost of fuel cell vehicles, without sacrificing performance.

II. MATERIALS AND METHODS

A. Fuel Cell Assembly

All single cell fuel cells comprise nine layers, as shown in Figure 1. The anode side consists of stainless steel end plate, gold-plated copper current collector, poco-graphite flow field, and a Teflon gasket. The cathode side is a mirror of the anode. In between the two sides is the MEA. The 50 cm^2, five-layer MEAs were supplied by GM. They consisted of cathode and anode gas diffusion layers and electrodes encasing a Nafion® PEM. The cells were assembled and incrementally compressed to 40 lb·in using bolts and a combination of standard and belleville washers. This ensured uniform contact throughout the components of the cell.
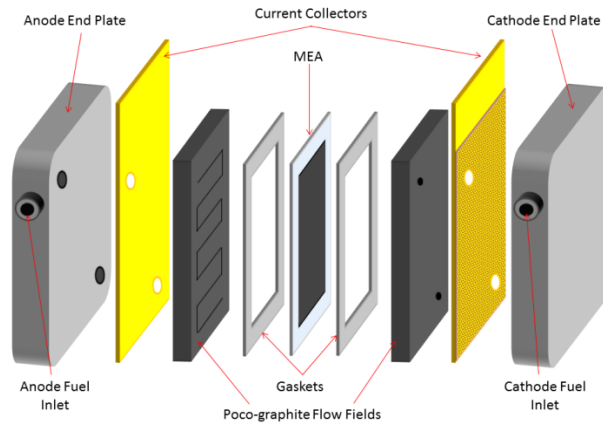
Figure 1. Fuel cell components.

B. Contaminant Details

The contaminant solution provided by GM was a leachate from a PPA structural material. This specific PPA material was one in a series of structural materials that were put through a leaching process to determine potential for membrane contamination. The American Society of the International Association for Testing and Materials (ASTM) D5336 defines PPA as a modified polyamide (PA = nylon) that must contain at least 55 Molar % of specific aromatic acids, as shown in Figure 2.
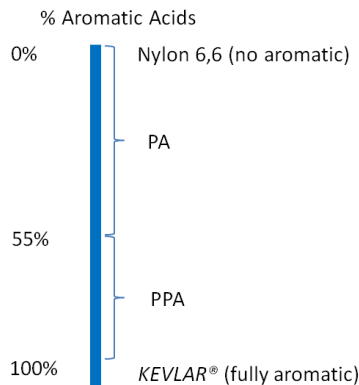
Figure 2. PPA is a modified PA that contains at least 55 % of aromatic acids.

Contaminant materials were leached by soaking the PPA in deionized (DI) water for 1000 hours at 90°C. A surface area to water volume ratio of 1.5 cm^2/mL was used in all leaching experiments to ensure a consistent amount of material surface available for leaching. After the leaching process the water was decanted and stored separate from leachate material to eliminate further leaching from the PPA material. The identity and quantity of the species in the leachate solution were determined using several analytical techniques: pH, solution conductivity, total organic content (TOC), ion chromatography (IC), and inductively coupled plasma (ICP). Figure 3 shows that the 2015 PPA material is much cleaner than the 2010 PA material (25x lower in TOC + conductivity), as shown by the lower anion and elemental concentrations.
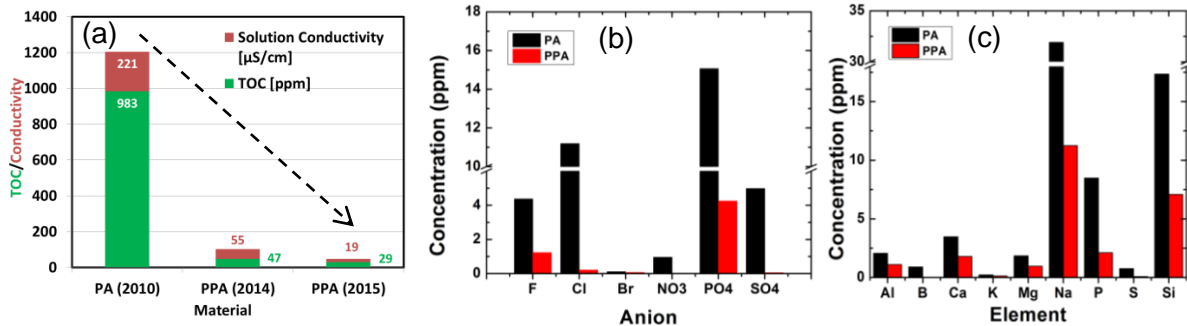

Figure 3. Characterization of PPA leachate solution (a) TOC and conductivity of different generations of PPA materials (2010, 2014, 2015). (b) IC results showing the anion concentration of the material leachates. (c) ICP results show the concentration of each element identified in the material leachates.

To understand PPA's effect on fuel cell performance, the PPA leachate was infused into the cathode using perfluoroalkoxy (PFA) tubing connected to a nebulizer (ES-4040 PolyPro ST Nebulizer) and a high performance liquid chromatography (HPLC) pump (LabAlliance™ Series III Digital Pump). The nebulizer ensured a fine aerosol of contaminant throughout the flow of air during the infusion experiment.
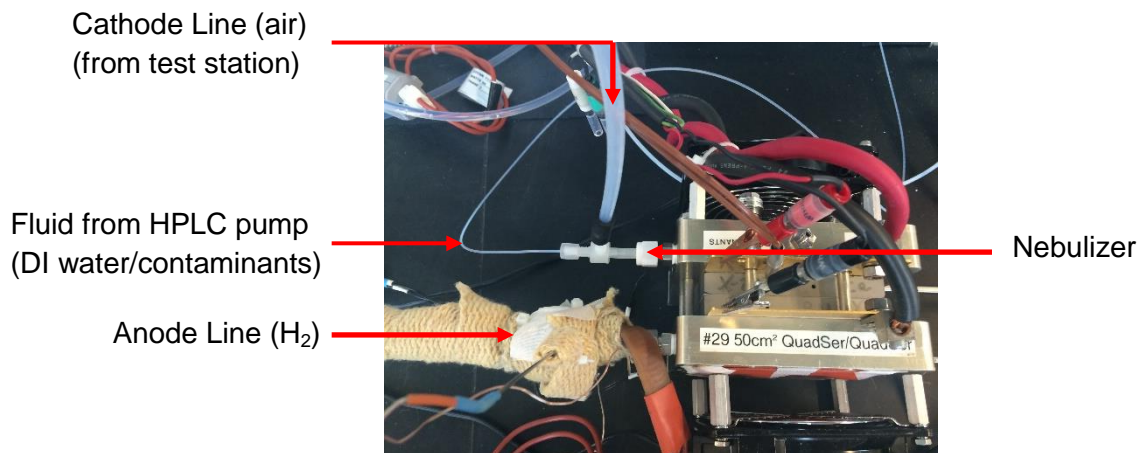

Figure 4. Infusion experimental setup[3] showing line and nebulizer connections to the fuel cell cathode.

C. Instrument Configuration

A Teledyne Medusa Fuel Cell Test Station and a Scribner 890e Fuel Cell Multi Range Test Load were used to perform *in situ* diagnostics on the fuel cells with High Frequency Resistance (HFR) being measured at 2.55 kHz. During infusion an Autolab potentiostat (PGSTAT302N) was used to carry out cyclic voltammetry (CV) and H_2/N_2 electrochemical impedance spectroscopy (EIS).

D. Experimental Procedure

The procedure used includes three main sections: Beginning of Life (BOL), Beginning of Test (BOT), and End of Test (EOT). These sections determine if an MEA is fit for testing, record a baseline of MEA performance before contaminant infusion, and then characterize the effects of contaminants after infusion, respectively. Operating conditions are given in the order of anode/cathode. For example, 800/2600 sccm hydrogen/air implies that 800 sccm hydrogen is flowed through the anode and 2600 sccm air is flowed through the cathode.

1. Beginning of Life (BOL)

After the fuel cell is assembled as described in Section A, the cell is tested to verify it is fit for experiment and will produce relevant data.
These tests include a leak test, electrical short test, and hydrogen crossover test. These are performed according to a procedure used in previous fuel cell contaminant related studies[3].
An MEA that passes the three BOL tests is determined to be fit for performance and contaminant testing. The MEA then through a break-in process which involves ramping up the current density of the cell from 0.2 to 1.5 A/cm^2 while running hydrogen/air. Once the cell reaches the maximum current density, it is cycled between 0.05 and 1.5 A/cm^2 at humidified (100% relative humidity [RH]) and dry (32% RH) conditions. This cycle is performed at least twice, and occasionally more if the fuel cell performance continues to improve. This process hydrates the fuel cell and ensures it is at an optimum state to be tested.

2. Beginning of Test (BOT)

An MEA that has proved its integrity during the BOL tests moves on to BOT diagnostics. BOT includes CV, EIS, and polarization curves (VIR).
Pt CV signatures are unique and can be used to determine the effect of contaminants on the Pt catalyst as well as to determine the ECA. By integrating the hydrogen under potential deposition (HUPD) region, Equation 1, and a charge-to-area conversion factor of 210 μC/cm^2, we can calculate the ECA. CVs were run on both the anode and cathode at a scan rate of 20 mV/s. For each CV, three cycles were performed to determine steady state.

$$\text{ECA} \left(\frac{\text{m}^2}{\text{g}}\right) = \frac{\text{HUPD (A*V)}}{\text{Sweep rate} \left(\frac{\text{V}}{\text{s}}\right) * \text{Constant}\left(\frac{\mu\text{A*s}}{cm^2}\right) * \text{Cell surface area}\left(cm^2\right) * \text{Catalyst loading}(\frac{\text{g}}{\text{m}^2})} \quad \text{Equation 1}$$

VIR measures the performance of the fuel cell by measuring the cell voltage (V) and HFR of a cell at different current (I) densities (Figure 5a). Three types of VIRs are run in series:

dry H_2/air (32% RH), wet H_2/air (100% RH), and wet H_2/O_2 (100% RH). The current densities used in VIRs are 1.5, 1.0, 0.8, 0.6, 0.4, 0.2, and 0.05 A/cm^2. Wet H_2/O_2 VIRs had two additional current densities 0.04 and 0.02 A/cm^2 to help determine the catalytic activity of the oxygen reduction reaction (ORR). The cell was held at each current density for 15 minutes to ensure a steady state. Before moving on to the next current density, EIS was performed. After each VIR, a hydrogen takeover was performed in which H_2/N_2 flowed until the cell potential decreased to around 0.12 V. This ensured no remaining oxides were left on the catalyst that would disturb performance characterization of the proceeding VIR.

EIS is used to characterize the individual capacitance and resistances associated with different MEA components as well as kinetic and mass transport limitations of the ORR. EIS is performed during BOT and EOT VIR and the infusion measurements, over a range of frequencies (from 10000 to 0.1 Hz, 6 points/decade) and using a current perturbation amplitude of 10% of the current (Figure 5b).
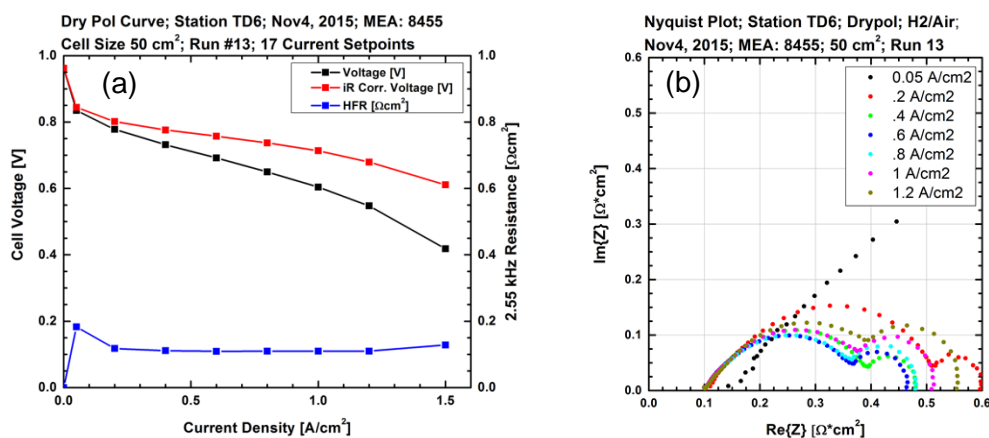

Figure 5. Example (a) VIR (pol curve) showing fuel cell performance and HFR. (b) EIS spectra measured during VIR at each current density step.

3. Infusion

Infusion was done by injecting either the humidified air or the PPA leachate solution into the air flowing to the cathode. This was done by bypassing the humidifier bottle in the test stand and replacing the cathode heated line with a nebulizer coupled with an HPLC pump. In order to have a baseline to compare the contaminant results to, DI water was infused with the air entering the cathode until the cell potential reached steady state (roughly 72 hours). Once steady state was achieved, the pump was switched from its DI source to the leachate solution. The contaminant infusion proceeded until steady state was reached, upon which a self-induced recovery (SIR) began by switching the infusion back from the contaminant solution to the DI solution. After infusion, the nebulizer was replaced with the heated cathode extension line and EOT began.

4. End of Test (EOT)

EOT includes the same diagnostics as BOT. EOT starts with half scan CVs between 0.05 and 0.5 V to determine the ECA without potentially removing contaminants that may have absorbed onto the catalyst surface during infusion. This is followed by VIR, H_2/N_2 EIS, full CV

scans between 0.05 and 1.0 V to clean the MEA of contaminants, an additional set of VIR, and the final H_2/N_2 EIS.

III. DATA ANALYSIS

EIS from VIR and infusion were analyzed using ZView-2 (Scribner Associates Inc.) software. Analyzing data in ZView 2 enables the isolation of different impedance factors in the fuel cell system. Isolation of resistance and capacitance values helps us locate and understand contamination effects.

Using ZView-2, EIS data were fit to equivalent circuit models that simulate the electrochemical systems. Because the EIS spectra were collected over a range of frequencies, we can attribute the different parts of the EIS spectrum to certain fast and slow processes in the fuel cell system. We validate the equivalent circuit models by fitting the impedance data collected under different conditions and best-fits are obtained.
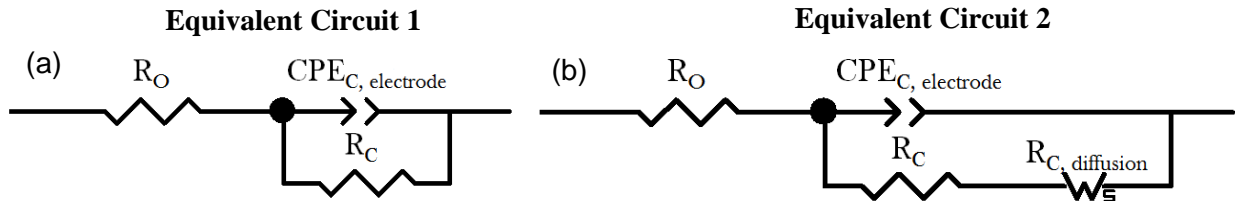

Figure 6. Equivalent circuit diagrams (a) Equivalent circuit 1 is used for fitting H_2/O_2 data. (b) Equivalent circuit 2 includes a diffusion component to more accurately model the impedance data in H_2/air experiments

H_2/O_2 data (blue curve in Figure 7a) show a semi-circle feature at intermediate frequencies (5 Hz to 1 kHz) and a high frequency intercept (~2.55 kHz) on the x-axis. Equivalent Circuit 1 was used to fit the H_2/O_2 data and Figure 7b (green curve) shows that the fit is very good. H_2/air data (black and red curves in Figure 7a) show two semi-circles and a high frequency intercept. The new semi-circle at low frequencies (0.1 Hz to 5 Hz) appears because of the diffusion of oxygen in air. Because of this new mass transport limiting process, a slightly different equivalent circuit (Equivalent Circuit 2) was used to fit the H_2/air EIS data. Again, Figure 7b (blue x curve) shows the fit is good.
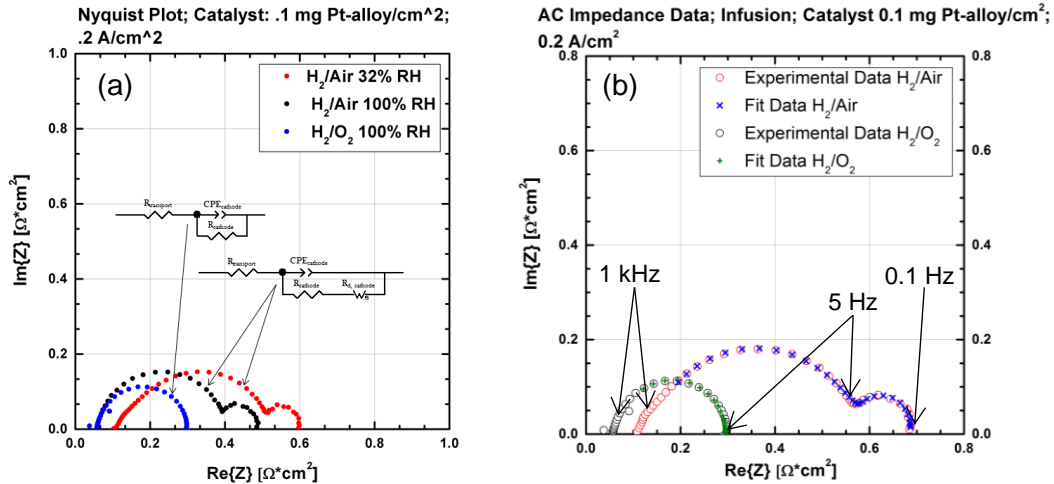
Figure 7. (a) Typical EIS curve for H_2/O_2 data (blue) was fitted to Equivalent Circuit 1. Typical H_2/air data (red and black) were fitted to Equivalent Circuit 2. (b) Good fits are shown for the H_2/O_2 and H_2/air EIS data.

The components of an equivalent circuit have physical meaning and they are shown by the schematics in Figure 8. The HFR, represented by R_O in the equivalent circuits, is attributed predominantly to the membrane conductivity (Figure 8a), but it also includes the interfacial and electronic resistances of the fuel cell assembly. R_C represents the charge transfer resistance of the ORR and is related to the kinetics of the reactions. $CPE_{C, electrode}$ represents the double layer capacitance of the porous conductive electrode (Figure 8b). The Warburg element (W_s), represented by $R_{C, diffusion}$, is the resistance of the oxygen molecules (in nitrogen) diffusing through a porous and tortuous path to the catalyst surface during H_2/Air ac impedance measurement[4] (Figure 8c).

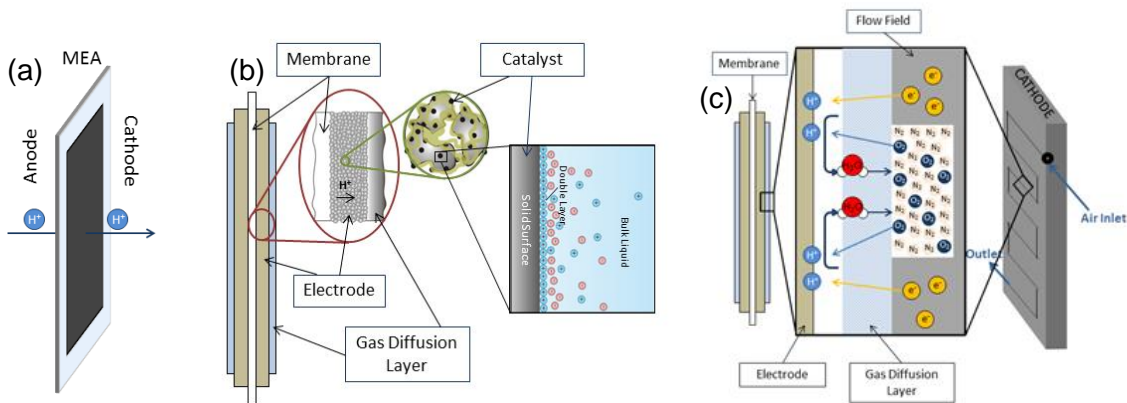Figure 8. Physical representations of resistance and capacitance effects in a cell (a) The resistance to proton transfer (membrane resistance) is the main contributor to HFR. (b) Double layer capacitance from layered cations and anions is shown on a cathode's catalyst layer. (c) Gas diffusion is represented inside a flow field through nitrogen molecules and the gas diffusion layer to the catalyst surface.

IV. RESULTS & DISCUSSION

Contaminant infusion was performed on a 0.1 mg/cm^2 Pt-alloy cathode using a PPA leachate solution provided by GM. The infusion was carried out at a constant current density (0.2 A/cm^2). The performance drop was measured by calculating the voltage loss (ΔV_1) between the measured voltage due to contamination and an extrapolated baseline[5]. During SIR, no contaminant was infused into the cathode for a period of time and the calculated ΔV_2 is the difference between the voltage loss after the SIR period and the extrapolated baseline.

Figure 9 shows that the PPA contaminant solution caused a voltage drop of $\Delta V_1 =$ 21.2 mV after 19 hours of infusion. The majority of the fuel cell performance self-recovered after 28 hours of SIR, resulting in a voltage drop of only $\Delta V_2 = 2.2$ mV.
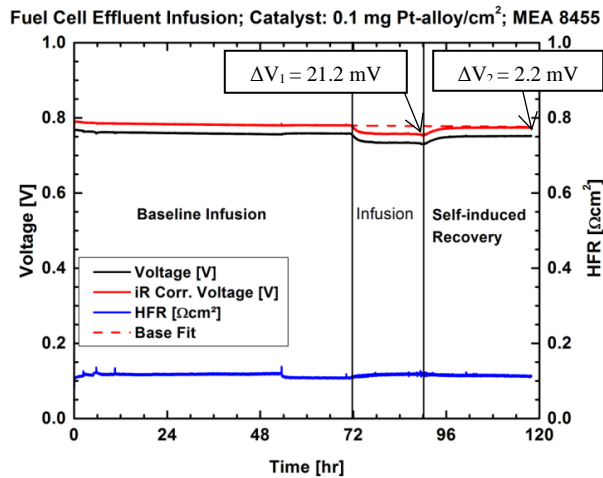

Figure 9. Fuel cell performance at 0.2 A/cm^2 and HFR over the course of the infusion experiment. A voltage loss of 21.2 mV was due to PPA leachate contamination infusion. After SIR, the voltage loss was only 2.2 mV, indicating that the majority of the performance has been recovered.

The Pt CV (Figure 10) indicates that the performance loss may be due to poisoning of the Pt-alloy catalyst. The red curve obtained after PPA infusion shows a 42% loss in active platinum sites (a drop from 47 m^2/g during baseline (black curve) to 27 m^2/g after infusion). Perhaps some anions and/or organics from the PPA leachate adsorbed onto the Pt surface and blocked the active sites. After some potential cycling between 0.05 and 1 V, the ECA regained up to 86% of its initial value (blue curve). It appears that potential cycling can help remove the adsorbed contaminants, but not fully. About 14% active surface area was still not recovered. Perhaps more potential cycling (> 3 cycles) or longer time of cycling can remove all of the adsorbed contaminants.
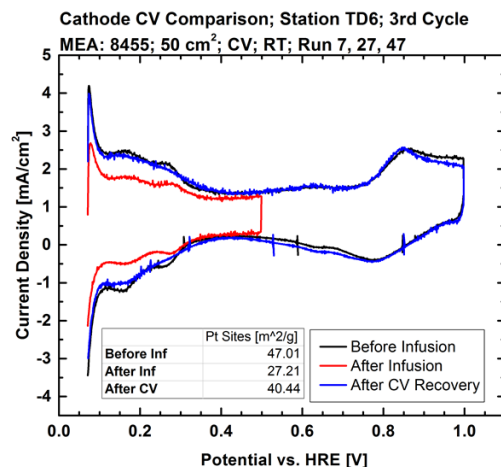
Figure 10. Pt CV taken on the cathode before infusion (black), after infusion (red), and after CV recovery (blue). The decrease in area after infusion shows that contaminants in the PPA leachate have blocked Pt sites.

Selected EIS data from the three phases of the infusion experiment (pre-infusion/baseline, infusion, and SIR) are shown in Figures 11 b-d. Pre-infusion impedance data stabilizes at about 20 hours into the baseline portion of the experiment. During the PPA leachate infusion, EIS spectra appear to shift to the right and the larger semi-circle seems to expand. Once infusion of contaminants stops (SIR phase), the EIS loops shrink and move left, resembling the initial shape obtained during pre-infusion.

Using Equivalent Circuit 2 to fit the EIS data, values for R_O, R_C, $R_{C, diffusion}$ and $CPE_{C,electrode}$ were extracted and plotted as a function of time (Figure 11e). R_O should have similar values as the HFR obtained from the VIR measurement because they both represent the membrane resistance. Because R_O was overestimated from our Equivalent Circuit 2 fit, we chose to plot the HFR data (blue) in Figure 11e instead of R_O. $R_{C, diffusion}$ (orange) and $CPE_{C, electrode}$ (not shown) remained constant at about 0.120 mΩ cm^2 and 0.02 mF/cm^2, respectively, throughout the experiment. HFR (0.108 mΩ cm^2) and R_C (0.385 mΩ cm^2) remained constant throughout the 70 hour baseline period. These values increased to 0.12 mΩ cm^2 and 0.433 mΩ cm^2, respectively, at the end of the infusion period. The increase in HFR indicates a decrease in the membrane conductivity, perhaps due to the cations in the PPA mixture reacting with the protons in the membrane. The increase in R_C indicates that a change in the kinetics of the ORR. During SIR, HFR and R_C decreased to 0.112 mΩ cm^2 and 0.395 mΩ cm^2, respectively. The good news is that the contaminants are not permanently altering the integrity of the cell or the electrochemical processes. Because if they were, the fuel cell would not likely recover to the extent observed.
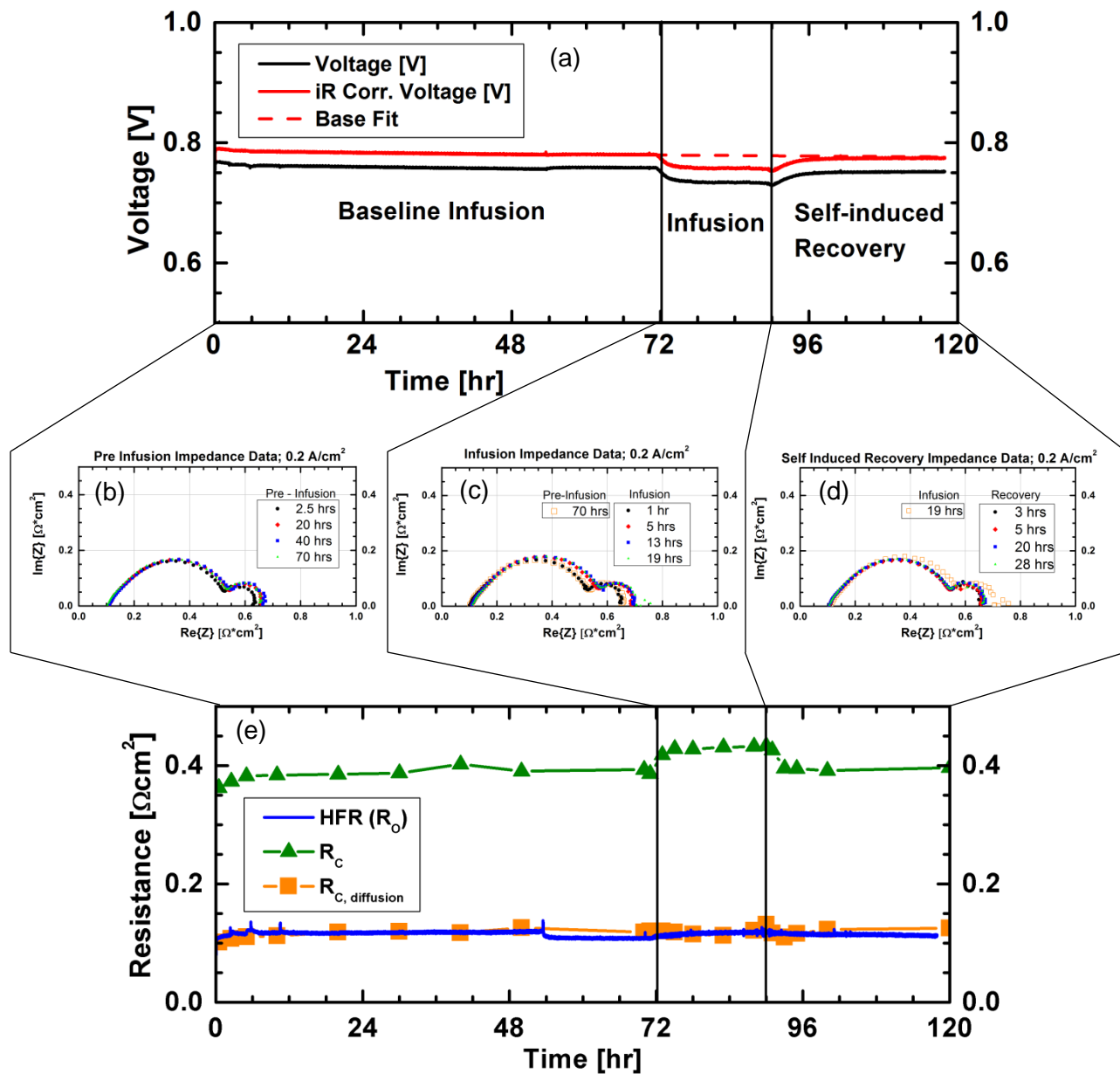
Figure 11. (a) H$_2$/air fuel cell performance measured as a function of time; (b) EIS data taken during pre-infusion or baseline; (c) EIS data taken during PPA leachate infusion; (d) EIS data taken during SIR. (e) R$_C$ and R$_{diffusion}$ values, extracted from fitting EIS data with Equivalent Circuit 2, plotted in conjunction with HFR, as a function of time during the three phases of the infusion experiment

Using Ohm's Law, the expected voltage drops from ΔHFR and ΔR$_C$ at the end of the infusion phase were 2.4 mV and 9.6 mV, respectively. The larger voltage drop due to R$_C$ indicates that it is the main cause for performance loss. Together, the change in these resistances accounted for 12 mV of the 21.2 mV measured for ΔV$_1$. This indicates that voltage loss due to the decrease in membrane conductivity and the increase in ORR charge transfer resistance do not

account for the total contamination voltage loss. There must be other impedance factors that we are not considering. Pt CVs above indicate that some of the voltage loss is due to adsorption of the contaminant species on the Pt sites. These species may be anions and/or organics. Contamination of the catalyst ionomer may also contribute to the overall voltage loss. Investigation into this additional factor will continue in further work.

V. CONCLUSION

The effect of the PPA leachate solution on the performance of a low loading Pt-alloy fuel cell cathode was studied. Results indicate that the contaminant solution primarily affected the performance of the cell by blocking Pt catalyst sites and a minor effect on membrane conductivity. The effect of the contaminant solution was not permanent and the fuel cell was able to recover. In addition to the effect on membrane conductivity and poisoning of the Pt catalyst, there are still other factors that need to be considered to fully account for the performance loss observed during the infusion of PPA solution.

Furthermore, an effective way to fit the ac impedance data was developed. Two equivalent circuits were found to fit the H_2/O_2 and H_2/air ac impedance data well and they were validated by the reasonableness of the values and the trends of the different resistance and capacitance components during the infusion experiment.

VI. FUTURE RESEARCH

While the two equivalent circuit models will continue to be used in the future to analyze impedance data, we will continue to develop our methods and increase the scope of our understanding of EIS data. This will be done by analyzing the H_2/N_2 and H_2/O_2 ac impedance data to determine the catalyst layer resistance due to ionomer poisoning.

To better understanding the contamination mechanism of the structural material leachate solutions on fuel cell performance, specific species from the PPA leached solution will be selected for further study. Because PPA is a mixture of contaminants from a structural material, it is very hard to pinpoint what species are causing the effects observed. Moving forward, we will pick a model compound like sulfate anion for further study. Sulfate anion is a good model compound to study because it can come from several sources, including the structural material, air, and the degraded membrane itself.

VII. AKNOWLEDGMENTS

VIII. APPENDICIES

Appendix A. Testing Procedure + Specifications

Table A1. Fuel cell component specifications

Cell Component	Anode	Cathode
Endplate material	Stainless steel	Stainless steel
Current collector material	Gold plated copper	Gold plated copper
Flow field area	50 cm^2	50 cm^2
Flow field material	Graphite	Graphite
Flow field channel	Double Serpentine	Triple Serpentine
Electrode area	53.29 cm^2	53.29 cm^2
GDL	Carbon Paper MRC-105	Carbon Paper MRC-105
Gasket	Teflon, 7 mil	Teflon, 8 mil

Table A2. Standard NREL break in procedure (RH = relative humidity, sccm = standard cubic cm, RT = room temperature, An = anode, Cat = cathode)

			NREL Standard Break-In Procedure			
Steps	Duration [s]	CD [A/cm²]	Temp [°C]	P [kPa]	RH [%]	Stoich. [An/Cat]
1	6	OCV	80	150	100	1.5/2
2	180	0.6 V	80	150	100	1.5/2
3	240	0.40	80	150	100	1.5/2
4	180	0.05	80	150	100	1.5/2
5	240	0.60	80	150	100	1.5/2
6	180	0.05	80	150	100	1.5/2
7	240	0.80	80	150	100	1.5/2
8	180	0.05	80	150	100	1.5/2
9	240	1.00	80	150	100	1.5/2
10	180	0.05	80	150	100	1.5/2
11	240	1.20	80	150	100	1.5/2
12	**40**	**OCV**	**80**	**150**	**100**	**1.5/2**
13	**180**	**0.05**	**80**	**150**	**100**	**1.5/2**
14	**240**	**1.50**	**80**	**150**	**100**	**1.5/2**
_15_	_30_	_OCV_	_80_	_150_	_32_	_1.5/2_
_16_	_180_	_0.05_	_80_	_150_	_32_	_1.5/2_
_17_	_240_	_1.50_	_80_	_150_	_32_	_1.5/2_
_18_	_40_	_OCV_	_80_	_150_	_100_	_1.5/2_
_19_	_180_	_0.05_	_80_	_150_	_100_	_1.5/2_
_20_	_240_	_1.50_	_80_	_150_	_100_	_1.5/2_
Repeat x10	_Repeat x6_	_Repeat x7_				

Table A3. Beginning of Life (BOL) procedure and conditions

Beginning of Life								
Test	Gas [An/Cat]	Gas Flows [An/Cat] [sccm]	RH [%]	Cell Temp [°C]	Pressure, Abs. [kPa]	Gas Stoichiometry [An/Cat]	Current Density [A/cm²]	Potential Range [V]
Leak Test	Air/Air			RT	207	N/A	N/A	N/A
Electrical Short	N_2/N_2	200/200	100	RT	Ambient	N/A	N/A	0-0.5
H2 Crossover	H_2/N_2	200/200	100	RT	Ambient	N/A	N/A	0-0.5
Break-In	H_2/Air	LEF		80	150	1.5/2	0-1.5	N/A

Table A4. Beginning of Test (BOT) procedure and conditions

Beginning of Test								
Test	Gas [An/Cat]	Gas Flows [An/Cat] [sccm]	RH [%]	Cell Temp [°C]	Pressure, Abs. [kPa]	Gas Stoichiometry [An/Cat]	Current Density [A/cm²]	Potential Range [V]
CV-Cathode	H_2/N_2	200/0	100	RT	Ambient	N/A	N/A	0.07-1.0
Impedance	H_2/N_2	200/200	100	RT	Ambient	N/A	N/A	0.2 0.45 0.9
CV-Anode	N_2/H_2	0/200	100	RT	Ambient	N/A	N/A	0.07-1.0
Dry Pol Curve	H_2/Air	LEF	32	80	150	1.5/2	0-1.5	N/A
Wet Pol Curve	H_2/Air	LEF	100	80	182	1.5/2	0-1.5	N/A
Wet Pol Curve	H_2/O_2	LEF	100	80	182	1.5/2	0-1.5	N/A
CV-Cathode	H_2/N_2	200/0	100	80	Ambient	N/A	N/A	0.07-0.5 0.07-1.0 0.07-0.5
Impedance	H_2/N_2	200/200	100	80	Ambient	N/A	N/A	0.2 0.45 0.9
CV-Anode	N_2/H_2	0/200	100	80	Ambient	N/A	N/A	0.07-0.5 0.07-1.0 0.07-0.5
H2 Crossover	H_2/N_2	200/200	100	80	Ambient	N/A	N/A	0-0.5

Table A5. End of Test (EOT) procedure and conditions

End of Test								
Test	Gas [An/Cat]	Gas Flows [An/Cat] [sccm]	RH [%]	Cell Temp [°C]	Pressure, Abs. [kPa]	Gas Stoichiometry [An/Cat]	Current Density [A/cm²]	Potential Range [V]
CV-Cathode	H_2/N_2	200/0	100	RT	Ambient	N/A	N/A	0.07-0.5
CV-Anode	N_2/H_2	0/200	100	RT	Ambient	N/A	N/A	0.07-0.5
CV-Anode	N_2/H_2	0/200	100	80	Ambient	N/A	N/A	0.07-0.5
CV-Cathode	H_2/N_2	200/0	100	80	Ambient	N/A	N/A	0.07-0.5
Dry Pol Curve	H_2/Air	LEF	32	80	150	1.5/2	0-1.5	N/A
Wet Pol Curve	H_2/Air	LEF	100	80	182	1.5/2	0-1.5	N/A
Wet Pol Curve	H_2/O_2	LEF	100	80	182	1.5/2	0-1.5	N/A
Impedance	H_2/N_2	200/200	100	80	Ambient	N/A	N/A	0.2 0.45 0.9
CV-Cathode	H_2/N_2	200/0	100	80	Ambient	N/A	N/A	0.07-1.0 0.07-0.5
CV-Anode	N_2/H_2	0/200	100	80	Ambient	N/A	N/A	0.07-1.0 0.07-0.5
Dry Pol Curve	H_2/Air	LEF	32	80	150	1.5/2	0-1.5	N/A
Wet Pol Curve	H_2/Air	LEF	100	80	182	1.5/2	0-1.5	N/A
Wet Pol Curve	H_2/O_2	LEF	100	80	182	1.5/2	0-1.5	N/A
Impedance	H_2/N_2	200/200	100	80	Ambient	N/A	N/A	0.2 0.45 0.9
CV-Cathode	H_2/N_2	200/0	100	RT	Ambient	N/A	N/A	0.07-0.5
CV-Anode	N_2/H_2	0/200	100	RT	Ambient	N/A	N/A	0.07-1.0

Appendix B: Equations

Equation 1 (below) calculates in m²/g the electrochemically active surface area of Pt in the catalyst layer

$$ECA\left(\frac{m^2}{g}\right) = \frac{HUPD\ (A*V)}{Sweep\ rate\ \left(\frac{V}{s}\right)*Constant\left(\frac{\mu A*s}{cm^2}\right)*Cell\ surface\ area(cm^2)*Catalyst\ loading(\frac{g}{m^2})}$$

Equation 2 (below) was used to fit the baseline infusion curve

$$V_{Fit}(t) = p_1 * exp\left(-\frac{t}{p_2}\right) + p_3 + t * p_4$$

where parameters $p_1 \geq 0$, $p_2 > 0$, $p_3 > 0$, $p_4 < 0$.

IX. REFERENCES

[1] U.S. Drive, "Fuel Cell Technical Team Roadmap," 3 (2013).

[2] H. N. Dinh, G. Bender, C. Macomber, H. Wang, and B. Pivovar, "Effect of System Contaminants on PEMFC Performance and Durability," (2013).

[3] J. Przywara, "Effect of cathode catalyst loading and sulfate contamination on fuel cell performance" 3 (2015).

[4] Y. Zhai, K. Bethune, G. Bender, R. Rocheleau, "Analysis of the SO_2 Contamination Effect on the Oxygen Reduction Reaction in PEMFCs by Electrochemical Impedance Spectroscopy" Journal of The Electrochemical Society, **159**, B525 (2012)

[5] G. Bender, M. Angelo, K. Bethune, R. Rocheleau, "Quantitative analysis of the performance impact of low-level carbon monoxide exposure in proton exchange membrane fuel cells" Journal of Power Sources, **228**, 161 (2012).